

**ANALYSIS OF THE IMPACT OF A p53 MUTATION IN A HOMOGENEOUS
GENETIC BACKGROUND**

A Dissertation
Presented to
The Academic Faculty

by

Kirti Karunakaran

In Partial Fulfillment
of the Requirements for the Degree
Master of Science in the
School of Biological Sciences

Georgia Institute of Technology
May 2020

Copyright © 2020 by Kirti Karunakaran

**ANALYSIS OF THE IMPACT OF A p53 MUTATION IN A HOMOGENEOUS
GENETIC BACKGROUND**

Approved by:

Dr. John McDonald, Advisor
School of Biological Sciences
Georgia Institute of Technology

Dr. Matthew Torres
School of Biological Sciences
Georgia Institute of Technology

J. Leonard Lichtenfeld, MD, MACP
Deputy Chief Medical Officer
American Cancer Society

Date Approved: March 30, 2020

To the two strongest women in my life who have influenced and supported me.

First, to Dr. Nirmala K Murthy, who always pushes me to do the best as well as demonstrating that with hard work and determination, you can do anything. She is the first woman in my family to obtain a Ph.D. in science which inspired me to pursue biology.

Second, to the memory of Valsala Arackal, who taught me the importance of kindness and patience. Her values of strength and resilience have continued to encouraged me throughout my career in science.

ACKNOWLEDGEMENTS

First, I would like to thank my advisor, Dr. John McDonald. I joined his lab in 2019 and despite being a senior undergraduate, he still gave me a chance to learn from him. Through his guidance and help, I was able to be accepted as Georgia Tech's first 5 year BS/MS student in the School of Biological Sciences. It is with his support that I have grown as a scientist.

I would also like to thank three important women in the McDonald Lab. First, Dr. Lilya Matyunina who assisted me with completing my experiments and directly helped me with the RT-PCR. Next, I would like to thank Dr. Minati Satpathy who first taught me the skills I needed to complete my work as well as directly helped me with western blotting. Finally, I would like to thank Dr. L DeEtte Walker, who has been very supportive and always made sure that I had what I needed to succeed. Without the help of these women, I know for sure that I would not have been able to complete my thesis.

In addition, I am very grateful for the other members of my thesis committee, Dr. Matthew Torres and Dr. J. Leonard Lichtenfeld. Dr. Torres was my genetics professor and I still remember his class fondly. Even when I was struggling with concepts, I remember that Dr. Torres would always be open for questions. Dr. Len works at the American Cancer Society and my first encounter with him was getting his advice about medical school and research. Throughout the past few years, he has been very helpful and supportive of my endeavors, specifically by giving me his own insight into career aspects.

I am also very thankful for my close friends and colleagues that I have made in the past 5 years. I would like to thank all the other members of the McDonald lab from the Ph.D. Students to the Masters students. Even though they all were studying bioinformatics, they would always

be willing to help me. Outside of lab, I am very grateful for the close friends and roommates that I have had over the years. Many of them have been supportive in helping me, specifically always reminding me to persevere.

Lastly, I am forever indebted to my family, specifically my parents Abi Murthy and Karunakaran Rajasekharan. With their love and support, they have given me the opportunity to succeed and chase my dreams. In addition to my parents, I am very thankful for my uncle, Dr. Siva Murthy, who would always be available for me to talk to and was able to give constructive feedback due to his knowledge of the field. I am also very grateful for my sister, Amita, who has been assisting me with school from the beginning.

TABLE OF CONTENTS

ACKNOWLEDGEMENTS	iv
LIST OF FIGURES	vii
LIST OF SYMBOLS AND ABBEVIATIONS	viii
SUMMARY	ix
CHAPTER 1. Introduction	1
CHAPTER 2. Material and Methods	7
2.1 Determining CRISPR-Cas9 Target Location	7
2.2 Cell Lines	8
2.3 Mutated Cell Lines	8
2.4 Single Cell Colonies and Mutated Strains	10
2.5 DNA Extraction	11
2.6 Alignment and Protein Translation	11
2.7 Western Blot	12
2.8 RNA Structure Prediction	13
2.9 RT-PCR	13
2.10 Growth Study Protocol	13
2.11 Cell Viability Assay	14
2.12 Statistical Analysis	15
CHAPTER 3. Results and Discussion	16
3.1 Creation of Successful Strain with p53 Deletion Mutation through CRISPR-Cas9 (Aim 1)	16
3.2 Protein and Gene Expression Levels in Wildtype and Mutated Cell Lines (Aim 2)	18
3.3 Growth Rate and Relative Apoptotic Function Comparison between Wildtype and Mutant Cell Lines (Aim 3)	22
3.4 LOF Mutation Created in p53 Gives Predicted Results	25
CHAPTER 4. Conclusions	27
REFERENCES	28

LIST OF FIGURES

Figure 1 – Guide RNAs used to target exon 4 of p53.	10
Figure 2 – Alignment of mutant cell lines at CRISPR-Cas9 targeted site.	16
Figure 3 – Full DNA alignment flanking target site with amino acid sequence.	17
Figure 4 – Protein expression under normal conditions of mutant and wildtype compared.	19
Figure 5 – RNA secondary structure prediction of deletion region	20
Figure 6 – Normalized RNA expression for wildtype versus mutant cell lines	21
Figure 7 – Growth rates for mutant versus wildtype.	22
Figure 8 – Wildtype versus mutant comparison for cell viability under different treatments of Cisplatin.	24

LIST OF SYMBOLS AND ABBREVIATIONS

Cas9	CRISPR Associated Protein 9
CDGs	Cancer Driver Genes
CDKs	Cyclin-Dependent Protein Kinase
CDK9	Cyclin-Dependent Protein Kinase 9
CRISPR	Clustered Regularly Interspaced Short Palindromic Repeats
DNA	Deoxyribonucleic Acid
gRNA	Guide RNA
IARC	International Agency for Research on Cancer
LOF	Loss of Function
MAPK	Mitogen-Activated Protein Kinases
MDM2	Mouse Double Minute 2/ E3 ubiquitin-protein ligase
MFE	Minimum Free Energy
nM	Nanomolar
PAM	Protospacer Adjacent Motif
PBS	Phosphate-Buffered Saline
PCR	Polymerase Chain Reaction
pTEFB	Positive Transcription Elongation Factor
RNA	Ribonucleic Acid
RTPCR	Real-Time Polymerase Chain Reaction
Seq	Sequence
SNPs	Single Nucleotide Polymorphisms
TBST	Tris-Buffered Saline-Tween
TP53	Tumor Protein 53
μ M	Micromolar
WT	Wildtype

SUMMARY

In more than 50% of cancers, p53, a tumor suppressor gene involved cell cycle arrest and apoptosis, has been seen to be heavily mutated making it an important gene to study. There are several studies on p53 and its role in cancer, but they ignore the impact of genetic background. Past studies have shown that genetic background can have a significant effect on the phenotypic consequences of cancer driver mutations, however, all these studies are carried out in a heterogeneous environment. The goal of my study was to utilize the CRISPR Cas 9 system to create a loss of function mutation in the p53 gene in a well characterized human cell line (HEYA8F8) and to evaluate the impact of this mutation on cell growth and apoptotic function in identical genetic backgrounds. The resulting mutation was a deletion in codons 33-36 of exon 4 which decreased the length of the protein from 393 to 389 amino acids. Using the cell lines with the specified deletion, growth rates over 96 hours were compared, which resulted in higher cell counts for the mutant in comparison to the wildtype. Assay for drug sensitivity using cisplatin, the standard of care for many cancers, showed that mutant cell lines had decreased apoptotic function (higher cell viability) in comparison to the wild type. The overall results demonstrated that mutations in p53 increase cell viability when treated with chemotherapy and an increase in cell proliferation. We believe that the cell lines with the loss of function mutations in p53 generated will provide an ideal experimental set up to study how the genetic background can evolve to enhance cancer in future studies.

CHAPTER 1. INTRODUCTION

Cancer, a collection of diseases caused by malfunctioning cells, is the second leading cause of death worldwide (WHO, “Cancer”, 2020; NCI, “What is Cancer?”, 2015). Cancer arises from genetic mutations in cells and can occur almost anywhere in the body. The origin point of cancer cells helps distinguish different cancers from one another (NCI, “What is Cancer?”, 2015). Even similar categories of cancers can vastly differ making it a heterogeneous disease. Globally, one in six deaths is due to cancer; thus, the diseases' research is relevant to our lives.

A major question in cancer research is differentiating cancer cells from normal cells. In 2011, Hanahan and Weinberg proposed a list of ten hallmarks used to characterize cancer (2011). They defined a hallmark as “distinctive and complementary capabilities that enable cancer growth and metastatic dissemination.” These ten hallmarks form an organizing principle for understanding cancer as a disease.

These hallmarks help categorize cancer driver genes (CDGs): genes that are said to promote tumor growth (Bailey et al., 2018). Cancer driver mutations are said to give an advantage to cancerous cells, and it is suggested that 5-7 driver mutations are required for the formation of most cancers (Pecorino, 2016). One common CDG that is mutated in a majority of cancers is the p53 gene (Bailey et al., 2018). Upon observation, this gene is involved with two cancer hallmarks: sustaining proliferative signaling and resisting cell death (Rivlin et al., 2011).

The p53 gene is a tumor suppressor (Zilfou, 2009). Upon activation, p53 will hinder the formation of cancer cells. The gene works as a transcriptional regulator for growth arrest (sustaining proliferative signaling) and apoptosis (resisting cell death). More than 75% of mutations in cancers is due to an error in the p53 protein; hence, it is one of the most widely studied genes in the human genome (Muller & Vousden, 2013).

Classified as the “Guardian of the Genome,” p53 is considered a major part of tumor suppressive mechanisms (Yue et al., 2017). Located on chromosome 17, p53 encodes for a 393 amino acid long protein. This protein can be divided into four domains, each with its own function ranging from transactivation to DNA binding. Each domain has certain areas that are heavily mutated in a majority of cancer cases, defined as mutational hotspots (Hsu, 1991). The p53 gene is involved with transcriptional regulation with downstream targets, and its activity is regulated at the protein level rather than the gene expression level. In healthy and non-stressed cells, p53 protein levels are low due to its negative feedback loop with MDM2, a negative regulator of p53 (Harris, 2005). MDM2 works by attaching ubiquitin to p53 which marks it as a target to be degraded, leading to the overall decrease in p53 expression. In turn, p53 is a transcriptional activator for MDM2, creating a balanced system between these two proteins.

Under stress conditions, the most common being DNA damage, p53 is activated and stabilized through phosphorylation, acetylation, and methylation (Yue et al., 2017). Stabilizing p53 alters the structure to prevent it from binding to MDM2 and from being degraded.

The activation of p53 leads to the halting of the cell cycle or the activation of the apoptotic pathway (Levine, 1997). The decision of which pathway is taken is determined by the extent of DNA damage and the cellular stresses it releases (Harris & Levine, 2005). This decision makes p53 a gatekeeper for cells in the body.

All cells in the body undergo a process of growth through the cell cycle. In the cell cycle, there are several checkpoints in place to prevent irregular cells from duplicating. p53 is involved with two checkpoints in the S and M phases (Harris & Levine, 2005). Under low levels of DNA damage, p53 will activate its cell cycle arrest pathway. As a result, p53 will interact with proteins such as p21, a cyclin dependent kinase inhibitor. When active, p21 will inhibit cyclin dependent

kinases (CDKs) that are specifically involved with driving the cell into the next phase of the cell cycle. p21's interaction will halt the cell cycle in the S and M phase. While the cell cycle is halted, DNA repair mechanisms will be activated to fix the damage (Vugt, Bràs, & Medema, 2005). Once the damage is fixed, the cell will continue through the cell cycle as planned.

However, there are some instances in which the damage in the cell is too great and repair is impossible. When this occurs, apoptosis, or programmed cell death, is activated to remove the old and damaged cells (Pecorino, 2016). This process is highly conserved across organisms and is completed without damaging the surrounding cells. Apoptosis occurs with a set of signals that activates a signaling cascade, causing the cells' contents to shrink and to undergo phagocytosis, the engulfing of material for disposal.

p53 will activate the apoptotic pathway, or cell programmed death. In normal cells, a stress signal such as DNA damage will induce the apoptotic pathway (Pecorino, 2016). Once DNA damage is recognized, p53 is activated and stabilized. Functional p53 will then induce the expression of genes that encode for receptors that activate the caspase cascade such as Bax protein. Bax then activates the caspase cascade, which starts the shrinking of cell content and formation of apoptotic bodies to undergo phagocytosis. This cascading process leaves only healthy cells.

These pathways activated by p53 demonstrate its gatekeeper functions as a tumor suppressor (Zilfou, 2009). Both arresting the cell cycle and activating the apoptotic pathway are options that lead to cellular and genetic stability by ensuring that cells are fixed or killed if damaged beyond repair. Since p53 is such an important gatekeeper, it is unsurprising that p53 is highly mutated in cancer. In cancer, the p53 pathway is inhibited, which allows cancer cells to grow uncontrollably. This mutation prevents p53's ability to examine cells for abnormalities,

thereby preventing activation and proper function. Mutant p53 will not activate proteins such as p21, which inhibits cyclin-dependent kinases (CDKs) that are important for cell cycle continuation (Pecorino, 2016). Since CDKs are not inhibited, cell growth will continue despite DNA damage. In apoptosis, a mutation in p53 prevents the activation of the apoptotic pathway by not activating Bax. Since the Bax protein activates the caspase cascade in apoptosis, the removal of Bax allows for cancerous cells to avoid cell death despite being severely damaged. Even though cellular stress occurs, the mutation in p53 allows cancer cells to form and persist.

While cancer driver mutations such as p53 have been widely studied, understanding of how cancer forms is more complicated than just mutations in certain genes. In reality, several factors including mutations in cancer driver genes may increase the chance of cancer (Mittal, 2015). The interactions of other proteins, especially those upstream from p53, can impact cancer formation. These interactions and other genes that are not of special interest in a study are called genetic background. Studies have shown that genetic background and cancer driver genes can increase the chances of cancer (Balmain, 2002). Genetic background can have a significant effect on the phenotypic consequences of cancer driver mutations. Simply put, an organism's genetic background can impact how cancer forms and impacts the ability of cancer to gain functions that assist in the survival of cancer. For instance, Donehower et al. found that mice with different genetic backgrounds but infected with the same cancer cells have different rates of tumorigenesis (1993). Despite the same mutation and infection of cancer driver cells, the genetic background had an influence on the tumorigenesis of the different mice. A newer study called "The evolutionary history of 2,658 cancers" determined that early oncogenesis is limited to the cancer driver mutations (Gerstung et al., 2020). However, as time passes, mutations will occur in the genetic background of the cell. These mutations are suggested to enhance the effect of the cancer

driver mutations and are shown to shape how cancer evolves. These studies lead to the possibility that mutations in cancer driver genes do not create the full phenotypic effect of cancer and questions how much a mutation in a cancer driver gene affects cancer.

While there are several studies on the function of p53 in cancer, most of them only examine genes affected by p53 and ignore genetic background. Studies of p53 in a heterogeneous genetic background do give meaningful results, however heterogeneous background prevents the understanding of how genetic background impact cancer phenotypes. For instance, a study in different cell types with the same loss of function (LOF) mutation in p53 found some unexplained gain of function activities in terms of cell growth and apoptosis (Bossi et al., 2005). While the study was done with the same mutation, the different cell lines meant the comparison was between different genetic backgrounds. This study suggests that genetic background may lead to gain of function activities in cancer cells. Another more recent study examined the role of p53 isoforms, or p53 protein variants, in renal cell cancer prognosis (Florijan et al., 2019). This study compared p53 isoforms between different patients of renal cell cancer which demonstrated that p53 isoforms are differentially expressed depending on mutational status. While these studies have given us a better understanding of p53 and its function, these comparisons do not account for genetic background.

The goal of this study was to utilize the CRISPR-Cas9 system to create a loss of function (LOF) mutation in the p53 gene in a well characterized human cell line (HeyA8F8) and to evaluate the impact of this mutation on cell growth and apoptotic function in identical genetic backgrounds. The HeyA8F8 cell line contains functional “wildtype” p53 alleles, making it an ideal choice. To accomplish this study, the following specific aims were created. The first was to employ the CRISPR-Cas9 system to create deletion mutations in a functionally significant region

of the p53 gene in the HeyA8F8 cell line. Then the molecular impact (protein and RNA levels) of p53 deletion mutations were determined. Finally, growth rates and relative apoptotic function between the wildtype p53 and p53 deletion mutants were compared. We hypothesized that a deletion mutation in p53 will show decreased expression as well as impact growth function and apoptotic function. The expectation of this study is to further emphasize the impact of a mutation on p53 in cancer cells as well as to provide an experimental cell line that can be used in the future to study the development of genetic background changes that occur in cells subsequent to mutations in major oncogenes.

CHAPTER 2. MATERIAL AND METHODS

2.1 Determining CRISPR-Cas9 Target Location

Functionally significant TP53 mutations are distributed in all coding exons of the TP53 gene, with a strong predominance in exon 4-9 (Rivlin, Brosh, Oren, & Rotter, 2011). Each exon has certain points that are mutational hotspots, and these exons are seen to be heavily mutated in cancer (Hsu, 1991). While a majority of mutations have been seen in the DNA binding domain, recent research has found a high prevalence of mutations in exon 4 since it lies close to the central region of the gene involved in DNA specific binding (Shepherd, et al., 2000). Since exon 4 is part of the transactivating domain, which is a part of p53 that interacts with other proteins, focus was specifically directed to the beginning portion of exon 4. This portion of exon 4 contains a few sites where it interacts with other proteins, specifically serine 33. Past studies of serine 33 have identified it as a phosphorylation site. Serine 33 interacts with other protein kinases (a kinase enzyme that modifies other proteins by chemically adding phosphate groups) such as p38. p38, a stress-activated protein kinase, helps mediate apoptosis and phosphorylates p53 at serine 33. In a study by Yogosawa and Yoshida, inhibition of p38 showed a reduction in phosphorylation of p53 at serine 33 (2018). This reduction in phosphorylation led to a reduction of apoptosis, suggesting that p38 plays a role in p53 mediated apoptosis. Another study showed that cyclin-dependent kinase 9 (CDK9), a protein kinase involved in the regulation of transcription (DNA to RNA), was also found to phosphorylate p53 on serine 33 (Radhakrishnan et al., 2006). CDK9 is found to be a component of the positive transcription elongation factor (pTEFB) and also interacts with RNA polymerase II, which expresses genes involved with proliferation and cell survival. While these papers do not give precise biological reasons or roles for phosphorylation, they suggest that serine 33 is important for apoptosis and cell proliferation.

In addition to the functional significance of this area, according to Synthego, who provided the guide RNAs for the CRISPR-Cas9 system, this location was specifically chosen for its high on-target score and low off-target homology. The specificity and the functional significance suggested that this attack location would cause a unique deletion in the p53 gene.

2.2 Cell Lines

Even though p53 is seen mutated in several cancers, our study was based on the HeyA8F8 cell line, a derivative of the HeyA8 cells (Pellicciotta et al., 2013). The HeyA8F8 cell line was altered to include a luciferase enzyme that allows for non-surgery bioluminescence imaging in mice for pre-clinical studies (Satpathy et al., 2016).

All cells were maintained in a growth medium consisting of RPMI 1640 (cell culture media), fetal bovine serum, and antibiotic antimycotic solution, all from Corning Inc. Cells were grown in single layer cultures and were kept in an incubator at 37 degrees with 5% carbon dioxide.

2.3 Mutated Cell Lines

The HeyA8F8 cell line was genetically edited to create a functionally significant p53 mutation. Since the guide RNAs provided had a high on-target score and a low off-target homology, it was believed to be specific in its mutation. p53 was altered to create a deletion mutation in exon 4. Exon 4 was chosen due to its high prevalence of mutations in soft tissue sarcomas and its lack of knowledge (Das et al., 2007).

To create this deletion, CRISPR-Cas 9 was used. Clustered Regularly Interspaced Short Palindromic Repeats (CRISPR) are DNA sequences that are found in the genome of prokaryotic organisms and were first discovered in *Escherichia coli* (Ratan et al., 2018). Cas9 (CRISPR associated protein 9) is an endonuclease, an enzyme that cleaves both strands of DNA. To

determine cleavage location, guide sequences find a complementary match in the targeted DNA. This method of cleavage with a specific guide led scientists to test if this system could be implemented as a genome editing tool. The CRISPR-Cas9 system is made up of two parts, the Cas9 enzyme and the guide RNA sequence. The system works by inserting the CRISPR-Cas9 system into a cell with a specific guide RNA. In addition to the guide RNA, the protospacer adjacent motif (PAM) with 5'-NGG-3' sequence on the targeted DNA is required for cleavage (Takara, 2020). To initiate gene editing, the guide RNA will find a matching sequence and bind. This will activate the Cas9 enzyme to cleave the DNA a few base pairs upstream of the PAM sequence causing a double stranded break. There are two methods of DNA repair. One option is to use homology directed repair, which requires the use of a template. The template will provide a strand that will allow for repair of the gene. In this option, a template strand can be given a specific change or insertion that causes a change in the DNA sequence. The other option is non-homologous end joining. This method works by DNA attempting to fix the break without a template. Since there is a double stranded break, nucleotides near the break will be removed, and then the two strands will be glued together. In our experiment, we used CRISPR-Cas9 to cause a double stranded break in exon 4 that was fixed with non-homologous end joining, since no template sequence was provided. Using the protocol and guide RNAs from Synthego, the mutated cells were created using the Synthego CRISPR-Cas9 Gene Knockout Kit (2019). According to Synthego, this kit guarantees that at least 50% of alleles in the pool of cells should have been edited. Four different guide RNAs were used in separate experiments to maximize p53 knockout. The guide RNAs were set to bind at exon 4 with the PAM sequence located in codon 33 and 34 (Figure 1). Each different guide RNA was used in a separate experiment, increasing the possibility of creating cells with a LOF mutation in p53. Once cells were potentially mutated

with CRISPR-Cas9, they were examined using an Invitrogen Detection Kit to detect cleavage. This kit shows if the CRISPR-Cas9 system worked and gives an estimation of the system's efficiency.

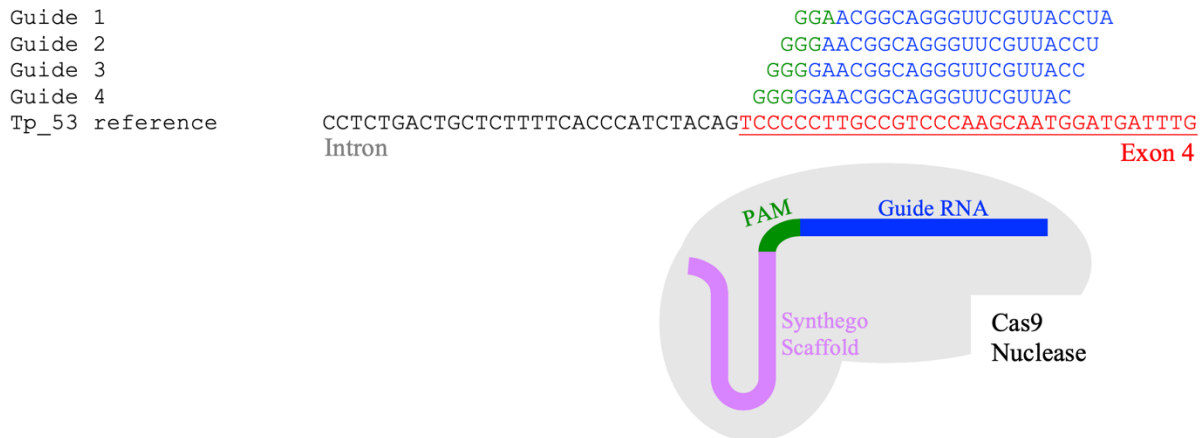


Figure 1: Guide RNAs used to target exon 4 of p53. Four guide RNAs from Synthego are shown in blue with the PAM sequence in green. Each gRNA met with Synthego's design criteria of early coding exon, common across all transcripts, high on-target score and low off target homology (Synthego, 2019). All four gRNAs were used in four different experiments of editing HeyA8F8 cells.

2.4 Single Cell Colonies and Mutated Strains

Once the detection kit showed results of cleavage, the mutated cell solutions were isolated to make single cell colonies. To create the different cell lines, clonal isolation was done. This was done by diluting the cells to a solution of 0.5-0.8 cells per 100uL. Then 100uL of the total solution was added to each well on a 96 well plate in the hope that only one cell would be in each well. From there, one single cell would divide and create its own colony. Once cells in a well seemed to be confluent, covering a majority of the cell surface, the cells were transferred to a larger cell plate until they were confluent enough to be put into a t-25 flask. Incubation of single cells to create new cell lines was only 24% successful. From successful colonies, we decided to focus on the following mutant strains: G1C4, G2C4, G3B2, G3C11, and G4F12.

2.5 DNA Extraction

After growing the single cell clones, their DNA was extracted and sent to be sequenced by Eurofins Genomics. While this did give sequencing results, this method did not provide clean sequencing results, suggesting single cell clones were not homozygous. The alternative method was to clone PCR product into a plasmid to obtain the sequence. Using PCR primers created to flank the targeted site in exon 4, the extracted DNA underwent PCR and the PCR product was then ligated into a plasmid that contained an antibiotic resistance aspect. This plasmid was then transfected into *E. coli* bacteria. After transfection, bacteria was plated and then treated with antibiotics. Since bacteria can only have one plasmid, only the bacteria with the plasmid that contains antibiotic resistance will survive. In addition to false positives, the PCR product was inserted into the LacZ gene, which normally gives bacteria a blue color. As a result, the bacteria with the plasmid and PCR product should be white colored bacteria. The white colored bacteria was then extracted and its DNA was isolated. The isolated product with primers in the genomic DNA that flanked the target site was sent to be sequenced at Eurofins Genomics. If all the sequences from the different populations had the same deletion, then the cell strain would be a homozygous population with a mutation in both alleles. However, if there were some sequences with deletion as well as some without deletions, this suggests that it was a heterozygous population and that the single cell colony was not correct. The results of the sequencing gave seq files of around 500 base pairs that could be aligned.

2.6 Alignment and Protein Translation

Using the obtained seq files, DNA sequences were aligned using Clustal Omega, which is a new multiple sequence alignment program that uses seeded guide trees and HMM profile-profile techniques to generate alignments between three or more sequences (Sievers et al., 2011).

The wildtype sequence was the HeyA8F8 cell line, and the mutant cell lines were those created using the CRISPR-Cas9 system. In addition, p53 sequence from the International Agency for Research on Cancer (IARC) were used as reference. The DNA sequences were then entered into ExPASy Translate tool which gave the protein sequence (Artimo, 2012). Final alignment in the 5' to 3' direction showed the primer sites, splice sites (pairs of bases that define the border between the intronic and exonic sequence for removal of introns) and exon regions with corresponding amino acids below with codon numbering. From the alignment file, one mutant strain (G3B2) was chosen to further study.

2.7 Western Blot

To determine the molecular impact of the deletion in p53, protein expression was measured. This was done using a Western Blot analysis. Cell lines were lysed in cell lysis buffer (CellLytic MT, Sigma) that contained protease inhibitors (Sigma) and were sonicated briefly. The sonicated precleared lysates containing proteins were then boiled in 4X sample buffer (Bio-Rad) and 2-mercaptoethanol. A Bio-Rad polyacrylamide gradient gel was loaded with the final solution. Gels were then transferred to a nitrocellulose paper and were blocked with 5% fetal bovine serum albumin in 10nM tris-buffered saline, pH 7.5, plus 1% Tween 20 (TBST, BioRad), for 1 hour at room temperature. The blots were probed with the following antibodies: p53 monoclonal antibody (Novousbio cat. no.NB200-103SS) and B-actin monoclonal antibody (Sigma, cat no 5441) diluted in 5% BSA in TBST overnight, with shaking at 4 °C. After incubation with the corresponding anti-mouse-horseradish peroxidase-conjugated secondary antibodies (Thermo Scientific Cat # 31430), the Western blots were developed by using the chemiluminescence technique (Pierce) according to the manufacturer's instructions. ImageJ was

used to quantify the protein expression values from the gel. Three different quantification methods of pixel density were used to compare statistical significance.

2.8 RNA Structure

To determine the possible effect of the deletion on RNA structure, RNAfold was used to predict the secondary structure using the Minimum Free Energy (MFE) method (2019).

Prediction software focused on the 500 base pairs that flanked the deletion region. Imaging and free energy values were taken and compared. Free energy values were calculated based on the paper by Zuker and Stiegler (1981).

2.9 RT-PCR

In addition to testing protein levels, we conducted real-time PCR with cyber green fluorescent dye to determine RNA expression levels. PCR data was collected following the BioRad protocol with six replicates per cell line, 3 for the target gene and 3 for the reference gene. GAPDH was used as the reference gene. The obtained data values were CT values, which is the number of cycles at which the fluorescent signal of the reaction crosses the threshold. Using the BioRad protocol for relative quantification between the target and reference as well as normalization of the data to the wildtype, fold expression was achieved. The fold expression was then averaged between the three replicates and standard error was found.

2.10 Growth Study Protocol

After identifying the molecular impact of the mutated cell lines, the growth rate of the mutant was compared to the wildtype. This was done by plating a number of cells and counting the cells at 24, 48, 72, and 96 hours. To examine growth rate, 100,000 cells per well were plated into a 12 well plate. Each plate was for one cell line and was divided by different time points. Each time point had 3 replicates. Cells adhered to the bottom of the flask. Thus, counting the

number of cells required resuspension of the cells. This was done by first washing the cells in PBS, using trypsin to detach the cells, and neutralizing the trypsin with growth medium. The cells were then centrifuged down and the liquid was aspirated, leaving a pellet of cells at the bottom of the tube. Cells were resuspended in 3-5ml of PBS to add to a hemocytometer for counting. Using both sides of the hemocytometer, the average for each section was taken and then multiplied by 10^4 to get the total number of cells per volume of PBS. The equation $C1V1=C2V2$ was then used as normalization to determine the number of cells per 1ml from the counted stock solution. The average of all replicates was then taken to give the number of cells for each 24 hour time point. This average was then graphed and standard error was calculated.

2.11 Cell Viability Assay

To test apoptotic function, cell viability under chemotherapy was completed. The standard of care for many cancers is Cisplatin, a platinum based drug that targets DNA in cells causing DNA damage (Dasari & Tchounwou, 2014). The hope is that Cisplatin will cause extreme DNA damage inducing apoptosis of the cell. Since DNA damage also activates p53, treating cell lines with cisplatin should demonstrate how this mutation impacts cell viability. The Cisplatin concentrations used were 0M, 1nM, 100nm, 1um, 10um, and 50um. Cisplatin concentrations were created by diluting a 2.67M stock solution. To test apoptotic function, a Sigma In Vitro Toxicology Assay Kit that is Resazurin Based was used. Resazurin is a blue fluorogenic dye that, in the presence of enzymes in viable cells, will change to create a red - fluorescence that can be detected spectrophotometrically in a BioTek Gen5 plate reader (O'Brien et al., 2003). Measurements are taken at time zero and every 30 minutes until all wells show a change in color. In a 96 well plate, 3,000 cells of the wildtype and mutant were plated in each well with 5 replicates for each concentration. 24 hours after plating, the media were removed

from each well and respective cisplatin concentrations were added to each well. 48 hours after adding the cisplatin medium, they were removed and the dye solution was added. The dye solution consisted of 10% of dye stock solution and 90% of cell culture media. Each well got 100uL of dye solution. The BioTek Gen5 plate reader gave absorbance values which averaged across all replicates and then were normalized to the 0M concentration value for each cell line. The normalized values were then multiplied by 100 to obtain percent values. Standard error was calculated across all replicates for each treatment and cell line.

2.12 Statistical Analysis

Determining statistically significant results between the wildtype and mutant cell lines in all experiments was done using a two-sample equal variance, one-tailed student's t-test. A p-value less than 0.05 was considered to be significant. Additional star markings indicated higher significance levels.

CHAPTER 3. RESULTS AND DISCUSSION

The goal of this study was to determine if a LOF mutation in p53 created by CRISPR-Cas9 to ensure identical genetic background demonstrated phenotypical differences in terms of cell growth and apoptosis. The overall results showed that a deletion in exon 4 encompassing the serine 33 phosphorylation site was consistent with previous findings in heterogeneous backgrounds — that this mutant is functionally significant.

3.1 Creation of Successful Strain with p53 Mutation through CRISPR-Cas9 (Aim 1)

To create the genetically identical mutants, we employed the CRISPR-Cas9 system to specifically target exon 4 of p53. Out of the colonies that grew successfully, we focused on G1C4, G2C4, G3B2, G3C11 and G4F12.

After DNA sequencing, we used Clustal Omega to align the five mutant strains, the HeyA8F8 wildtype, and IARC p53 reference sequence. Alignment showed mutant G2C4, G3B2 and G3C11 had a 12-nucleotide deletion in exon 4, while mutant G1C4 showed no difference (Figure 2).

	Splice Site
HeyA8F8 (Wildtype)	CCTCTGACTGCTCTTTTCACCCATCTACAGTCCCCCTTGCCGTCCCAAGCAATGGATGATTTG
G1C4	CCTCTGACTGCTCTTTTCACCCATCTACAGTCCCCCTTGCCGTCCCAAGCAATGGATGATTTG
G2C4	CCTCTGACTGCTCTTTTCACCCATCTACAG-----TCCCAAGCAATGGATGATTTG
G3B2	CCTCTGACTGCTCTTTTCACCCATCTACAG-----TCCCAAGCAATGGATGATTTG
G3C11	CCTCTGACTGCTCTTTTCACCCATCTACAG-----TCCCAAGCAATGGATGATTTG
tp53_reference	CCTCTGACTGCTCTTTTCACCCATCTACAGTCCCCCTTGCCGTCCCAAGCAATGGATGATTTG
	***** TCCCCCTTGCCGTCCCAAGCAATGGATGATTTG *****
	Exon 4

Figure 2: Alignment of mutant cell lines at CRISPR-Cas9 targeted site. Using Clustal Omega, all mutant cell lines were aligned to show possible mutations in target site of exon 4. Red indicates exon 4, grey highlights indicates splice sites, and stars indicate a consensus among all cell lines. Reference sequence was taken from IARC. G1C4, G2C4, G3B2 and G3C11 were single cell colonies grown after being edited with Synthego CRISPR-Cas9.

Sequencing and alignment of G4F12 was inconsistent, suggesting that the starting colony solution contained more than one cell or that the mutation created was not homozygous. Since mutants G2C4, G3B2 and G3C11 had the same alignment and deletion, they were consolidated

into one sequence file and renamed mutant. The wildtype, mutant and reference sequence were then all aligned and translated to include amino acids (Figure 3).

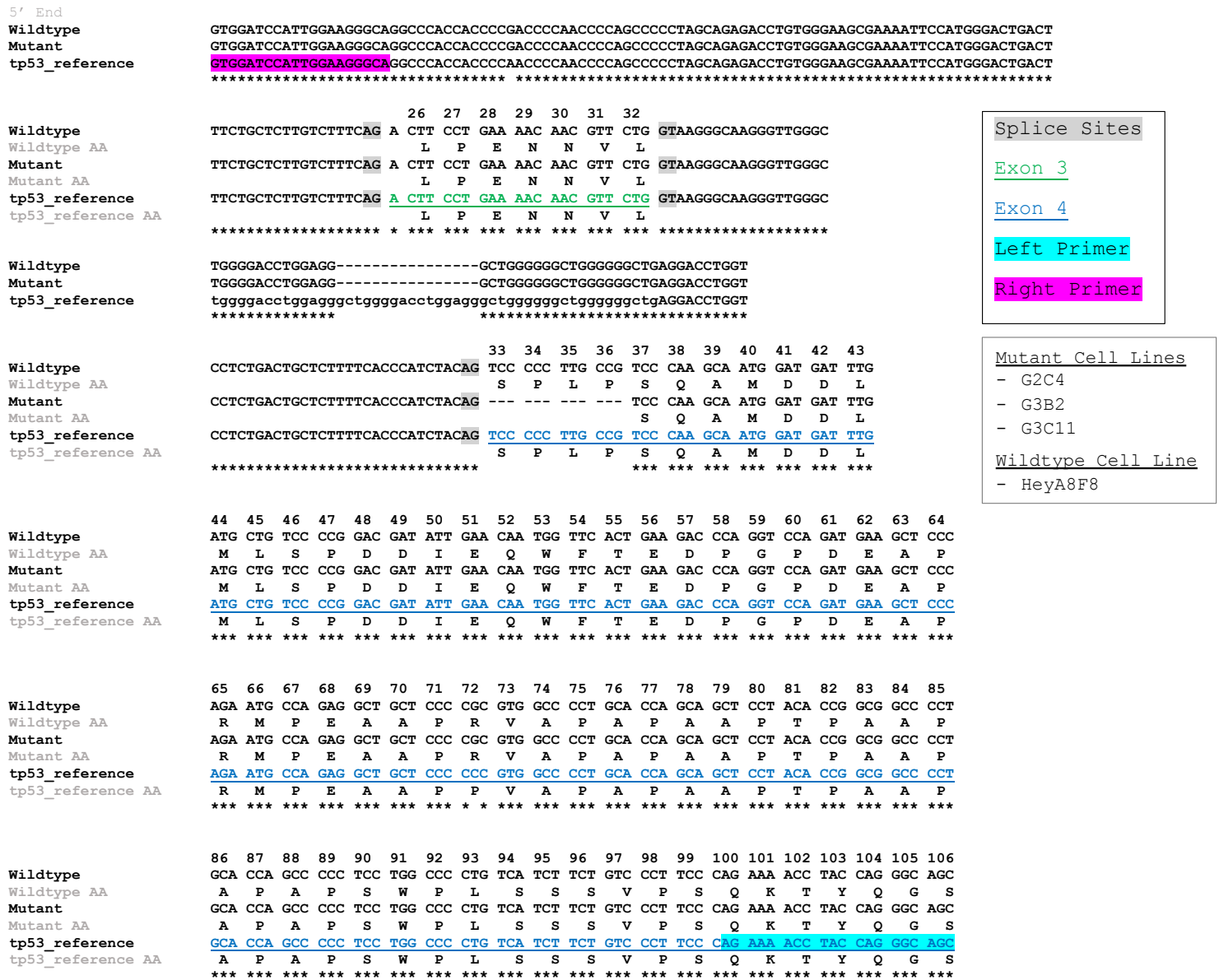


Figure 3: Full DNA alignment flanking target site with amino acid sequence. Sequences from Eurofins Genomics were aligned using Clustal Omega. Alignment is shown in the 5' to the 3' direction with the exonic regions underlined and primers and splice sites marked. Stars on the bottom are present where there is a consensus among all sequences. Amino acid sequence was translated from DNA sequence using ExPASy tool. Since mutant cell lines G2C4, G3B2, and G3C11 had the same deletion, a new sequence file labeled Mutant was used to represent all cell lines.

The most obvious dissimilarity seen between the mutant and the wildtype is the deletion at the beginning of exon 4, which consists of 12 nucleotide bases/4 amino acids and which includes serine 33. This deletion is only seen in the mutant. Since the deletion is exactly 12 amino acids long, there is no change in the reading frame. Instead, the p53 protein is shortened from 393 to 389 amino acids long. In comparison to the reference sequence, both the mutant and wildtype share a few other differences. Near the right primer, there is a G instead of an A. In addition, there is a deletion in both the mutant and wildtype cell lines in the intronic sequence between exons 3 and 4. Since these changes are in intronic regions, there should be no changes to the p53 protein. However, in the exonic region, both the wildtype and mutant share a single nucleotide polymorphism (SNP) in codon 72. This SNP leads to conversion of the amino acid from proline (CCC) to arginine (CGC). This conversion is important to recognize because proline is a neutral, nonpolar, but bulky amino acid while arginine is a basic amino acid. This change from neutral to basic can affect the structure of the protein, leading to a possible change in function. Recent studies in ovarian cancer demonstrated an association between this polymorphism and the risk of cancer development, along with a variation in the patient's response to chemotherapy (Antoun et al., 2018).

One study suggests that codon 72 as arginine is more effective in inducing apoptosis than proline, but states that the reason for this is not fully understood (Olivier, Hollstein & Hainaut, 2010). All these differences seen in both the wildtype and mutant further emphasize their identical genetic backgrounds. The only variation between the wildtype and mutant is the deletion in exon 4, suggesting that any significant differences would be caused by our CRISPR-Cas9 deletion.

3.2 Protein and Gene Expression Levels in Wildtype and Mutated Cell Lines (Aim 2)

After determining that a deletion mutation had occurred in the desired location, the molecular impacts, specifically protein and RNA expression, were compared to the wildtype. Since the mutants G2C4, G3B2 and G3C11 all showed the same deletion, we decided to focus on the G3B2 cell line. Since p53 is regulated at the protein level, we started with examining protein level through a western blot analysis. The western showed that the mutant G3B2 had decreased protein expression in comparison to the wildtype (Figure 4).

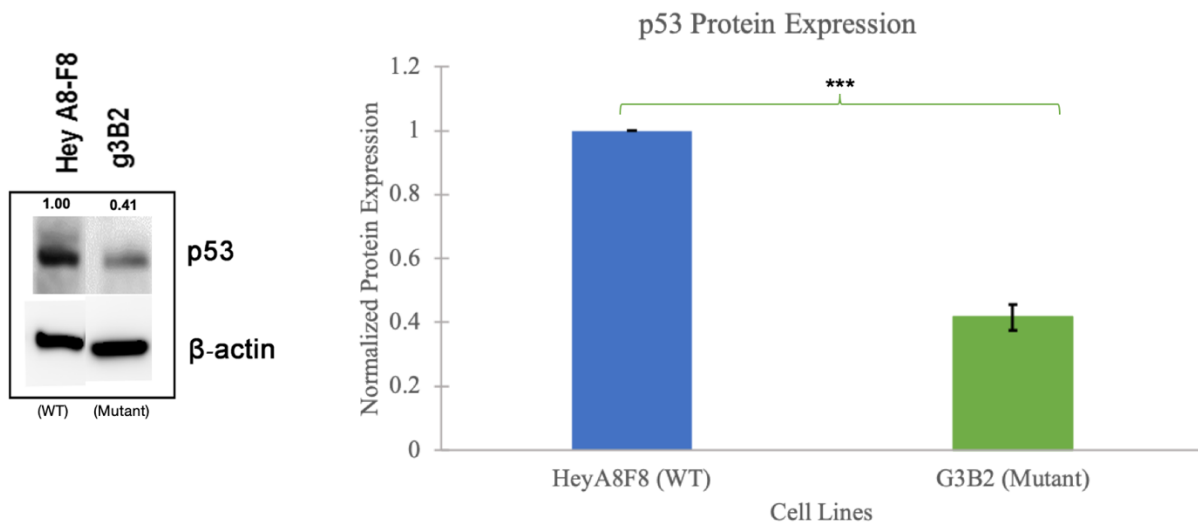


Figure 4: Protein expression under normal conditions of mutant and wildtype compared. A western blot analysis of p53 was completed using cell lysates and p53 monoclonal antibody (Novousbio cat. no.NB200-103SS), and B-actin monoclonal antibody (Sigma, cat no 5441). A picture of the gel is seen on the left. Quantification of the western blot was completed in ImageJ to show band intensity and shown on the right. Three different quantification methods of the pixel density completed in ImageJ gave standard error and two sample, equal variance student's t-test gave a p-value of 0.0001. *** indicates $p < 0.0005$

A two sample, equal variance student's t-test gave a p-value of 0.0001, which was considered to be statistically significant when compared to 0.05. Normally, p53 is seen at low levels in the cell and is degraded by MDM2. Phosphorylation of p53 activates the protein and increases its expression levels. Our mutant, normalized to the wildtype, showed lower expression. The deletion encompasses the serine 33 phosphorylation site, allowing for the protein to be degraded to lower levels than normal.

Even though p53 is regulated on the protein level, we did have a 12 nucleotide deletion in the DNA. This lead us to examine if there was a predicted change in the secondary RNA structure. Visual and free energy differences in the secondary RNA structure would give a possible explanation to differences seen in RNA expression. To determine the secondary RNA structure, RNAfold was used (2019). This site uses different methods to predict secondary RNA structure, however, we decided to focus on the Minimum Free Energy (MFE) method since it predicts structures based on lowest value of free energy. From RNAfold, a slight difference is seen visually (Figure 5).

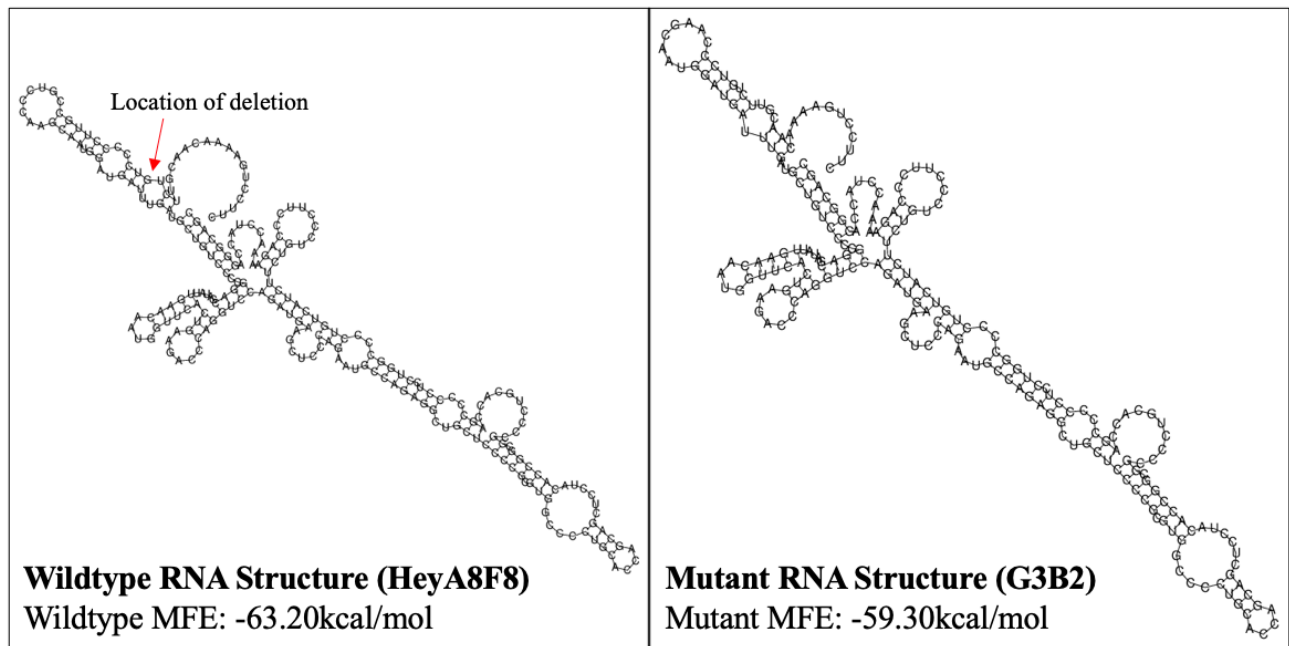


Figure 5: RNA secondary structure prediction of deletion region. *RNAfold*, a webserver that predicts secondary structures of RNA through minimum free energy(MFE), was used to visually compare the wildtype and mutant. The predicted free energy values are also shown for each image.

There is a slight difference in structure indicated by the arrow in Figure 5. In addition, the MFE values for the wildtype and mutant structure was -64.20kcal/mol and -59.30kcal/mol, respectively. MFE values can give a prediction of the stability of the RNA, with the lower value indicating the more stable RNA structure (Garcia-Martin & Clote, 2015). The wildtype had a

lower MFE value suggesting that it is more stable in comparison to the mutant, which may be reflected in RNA levels.

Since the mutant RNA was predicted to be less stable, we wanted to test to see if there was decrease in RNA expression as well. Using RTPCR, RNA expression was seen to be lower in the mutant than the wildtype (Figure 6). A two-sample equal variance student's t-test gave a p-value of 0.011 which is less than 0.05, suggesting a statistically significant difference.

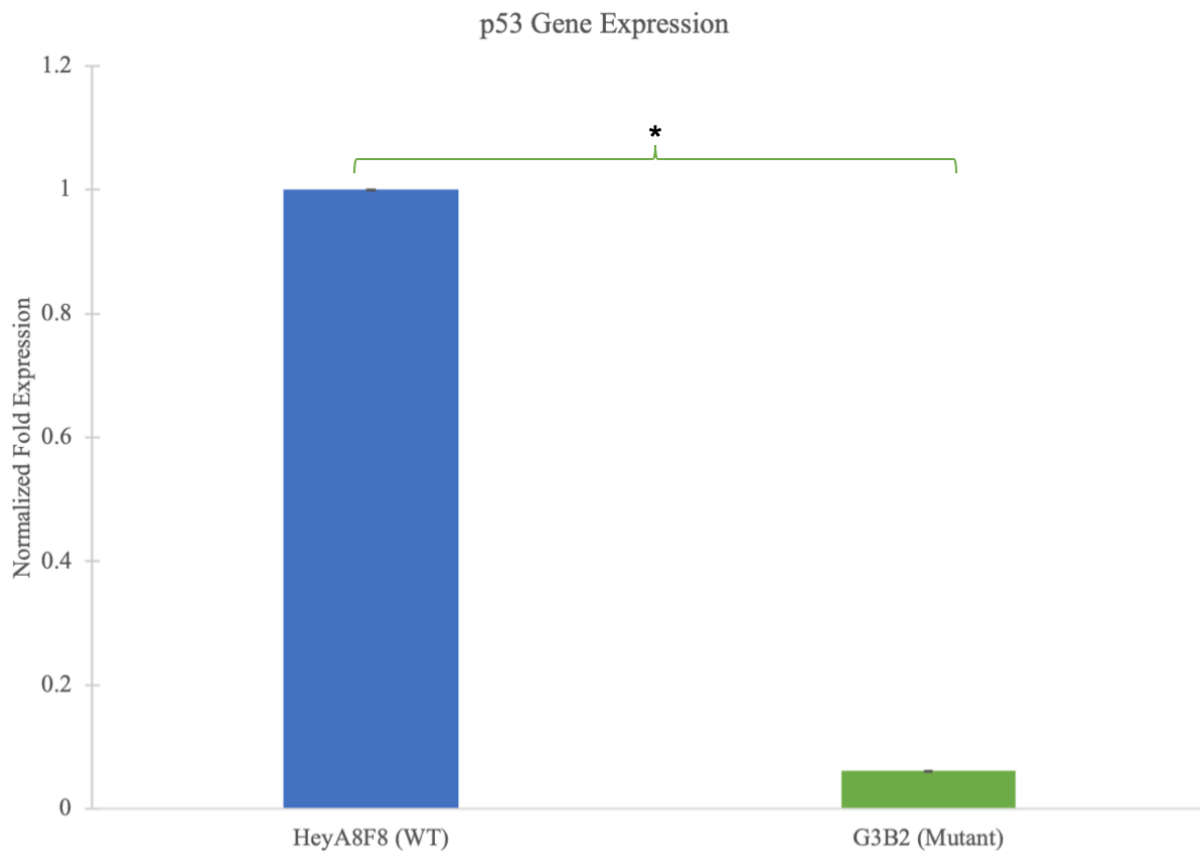


Figure 6: Normalized RNA expression for wildtype versus mutant cell lines. Following protocol provided by BioRad with cyber green fluorescent dye, CT values (number of cycles at which the fluorescent signal of the reaction crosses the threshold) were obtained. CT values were normalized to reference, GAPDH, and then normalized to the wildtype cell line. Standard error was calculated for all replicates. A two sample equal variance student's t-test was completed giving a p-value of 0.01 which is less than 0.05 and indicated by the *.

The decrease in RNA levels is consistent with the hypothesis that the deletion altered the RNA structure affecting RNA stability. RNA expression seems to be 10 fold lower while protein

expression closer to 4 fold decrease. The greater decrease in RNA could be due to the rate of degradation. RNA degrades much faster than protein. In addition, protein half-life can reduce the rate of degradation. The removal of serine 33 in p53 suggests a change in stability in both the protein and RNA level. Past studies of p53 have been done in different cell lines with large nonspecific deletion in the transactivating domain show similar results in protein and RNA levels (Zhu et al., 1998; Florijan et al., 2019). These results suggests that our mutation creates a LOF mutation in p53. Our study is the first study to report the effects of a deletion region containing this serine 33 site in terms of protein and RNA levels. This led us to test if p53 function in both cell cycle and apoptosis would be affected with the removal of this site.

3.3 Growth Rate and Relative Apoptotic Function Comparison Between Wildtype and Mutant Cell Lines (Aim 3)

With the knowledge that our deletion created a LOF mutation, we wanted to compare growth rates and relative apoptotic function between the wildtype and mutant. From the results of our growth study, we see that our mutant grew faster in the first 72 hours (Figure 7).

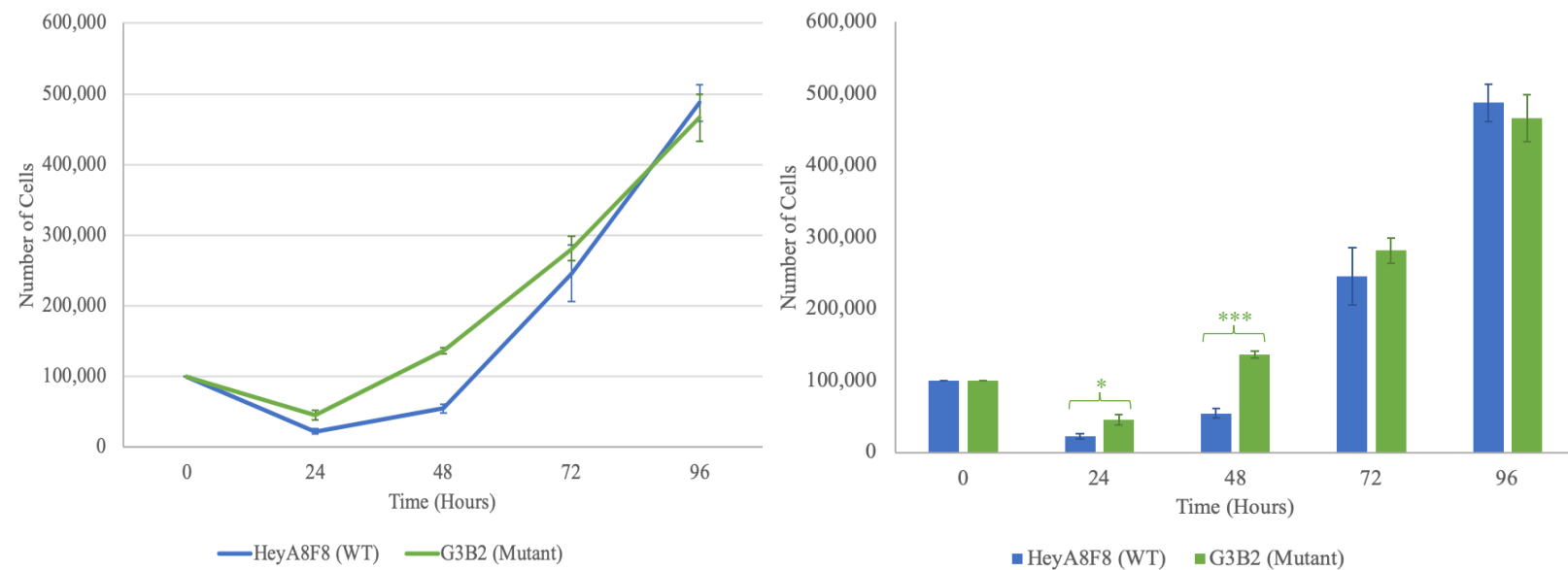


Figure 7: Growth rates for mutant versus wildtype. Cell proliferation was measured by plating 100,000 cells per well in a 12 well plate and were counted at the respected time points. Cell counts were normalized using $C1V1=C2V2$ and then averaged across all replicates. A two-sample equal variance, one-tailed student's t-test was completed to determine statistical significance. The p-value for 24 hours and 48 hours was 0.019 and 0.00053 respectively. * indicates p-value less 0.05, *** indicates p-value less than 0.0005.

At both 24 and 48 hours, the difference between the wildtype and mutant is statistically significant with a p-value of 0.019 and 0.00053 respectively. At 72 hours, we still see that the mutant is growing faster than the wildtype but the difference has decreased dramatically with overlapping standard errors. By 96 hours, no significant difference in growth rates between the two variants could be detected. We suspect that the reason for the slowing growth rates and the flip at 96 hours is due to the cells reaching confluency: cells have covered a majority of the well surface. We expect that if we continued measuring past 96 hours, we would see the growth rates leveling off.

Overall, our results show that there is a higher growth rate for our mutated cells. This matches the definition of cancer as uncontrollable growth. The expectation of cancer cells is to grow abnormally fast, which is why most therapies are aimed at all fast growing cells. In normal cells, p53 will prevent continuation of the cell cycle with stresses such as DNA damage. The cell cycle will only continue once these stresses are removed. However, by mutating p53, we are allowing cancer cells to evade the stress removal check point. The removal of this checkpoint allows for cells to move through the cell cycle at an abnormal rate that matches high growth rates. Our results are similar to past studies of p53 completed in heterogeneous backgrounds that show that growth rates are higher in mutants in comparison to wildtypes (Bossi et al., 2006; Ventura et al., 2007). For instance, one study showed that when they knocked down mutant p53 in cancer cells, growth rate and replication rate were seen to decrease. These results suggest that mutant p53 increases growth rate and removing it from the cell decreases growth rate. These studies demonstrate the importance of p53 in cell growth. However, our study is the first to show the solo effect of p53 without any genetic background influence.

After completing growth rates, we wanted to test cell apoptotic ability and viability under chemotherapy. The standard of care for many cancers is Cisplatin: a platinum based drug that damages DNA and inhibits DNA synthesis. Our test for apoptosis was a cell viability assay. The overall results of the test showed that the mutant cell line had higher cell viability (Figure 8).

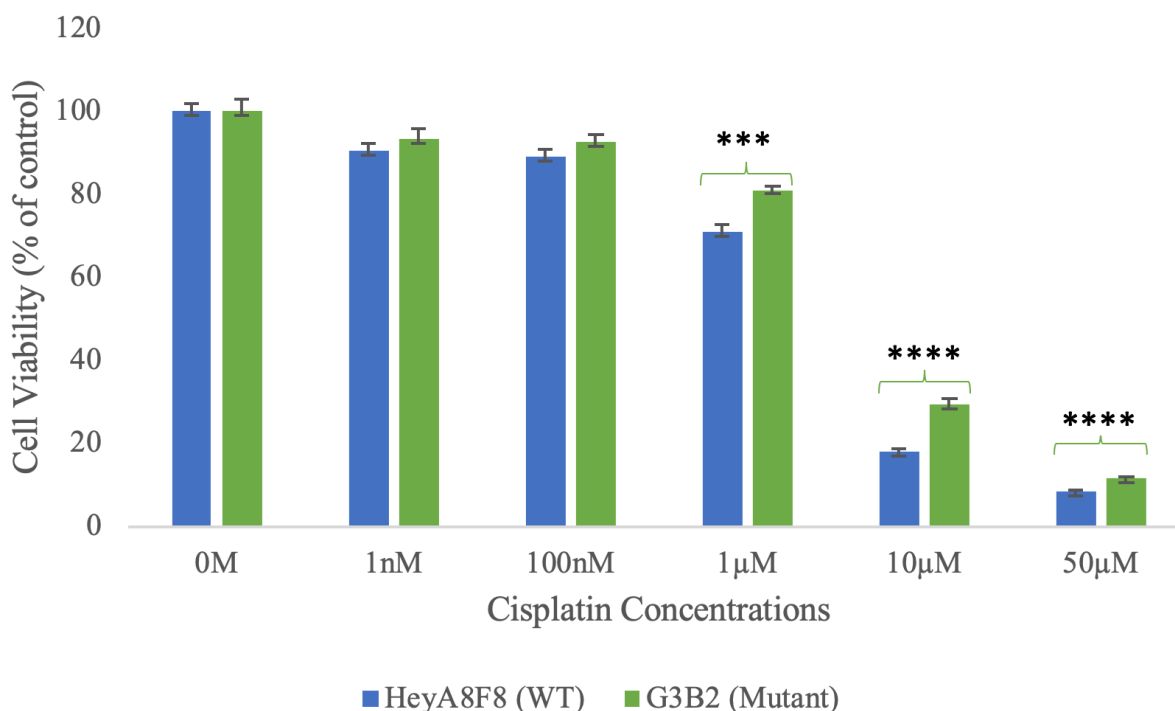


Figure 8: Wildtype versus mutant comparison for cell viability under different treatments of Cisplatin. Apoptotic function was tested using a Resazurin based Sigma In Vitro Toxicology Assay Kit. Cisplatin, the standard of care for ovarian cancer, was diluted from a stock solution to the following concentrations: 1nM, 100nM, 1μM, 10μM, and 50μM. Five replicates per treatment were done and seen in standard error. A two-sample equal variance, one-tailed student's t-test was completed to determine statistical significance. The p-value for 1μM, 10μM and 50μM was 0.00065, 0.000038 and 0.000043, respectively. *** indicates p-value less than 0.0005 and **** indicates a p-value less than 0.00005.

Higher cell viability indicates more live cells than dead cells. It is also described as decreased apoptotic function, meaning that apoptotic pathway is not activated or killing cells. At low levels of Cisplatin, we see high cell viability and low apoptotic function. When we increase the Cisplatin concentration, cell viability decreases as a result of severe DNA damage. However, cell viability is still higher in the mutant despite high levels of Cisplatin. These results are

consistent with past studies where p53 mutations decreased apoptotic function and increased cell viability (Brown & Wouters, 1999). In addition, our results are consistent with a previous study demonstrating the significance of phosphorylation of serine 33 in control of apoptotic function (Sanchez-Prieto et al., 2000). However, this past study examined apoptosis in regards to p38 inhibition while our study is in regards to p53 serine 33 deletion. This region is part of the transactivating domain of p53 with other amino acids important for phosphorylation. Understanding the complexities of this domain can further explain the importance of p53 activation. In addition, understanding p53 activation can give a biological explanation of what pathway p53 activates in terms of cell cycle or apoptosis. This is the first study for deletions in p53 mapping to serine 33 region in a genetically identical background.

A future study based on the effects of resistance to cisplatin would examine how mutant strains compare in terms of protein and RNA levels under chemotherapy. Treating cells with cisplatin concentrations, then following up with RT-PCR and western blotting, could give a better picture in terms of how cisplatin affects p53.

3.4 LOF Mutation Created in p53 Gives Predicted Results

Overall, the results of our study show that a LOF deletion mutation in p53 creates the predicted outcomes in our cells. We saw that our mutant had lower protein and RNA expression, higher growth rates, and higher cell viability when treated with Cisplatin. Our results are generally consistent with previous findings that p53 LOF mutations are functionally significant to growth rates and apoptotic function. However, we are the first to directly validate the functional importance of the serine 33 phosphorylation site in p53 gene with regards to identical genetic background. Mutations in p53 create the defined effects that is seen in cancer. In addition, these LOF mutations are of primary significance in creating cancers. The results of our

experiments can be clearly attributed to the created mutation without any influence from the genetic background.

However, a limitation of our study was that comparisons were completed only using the G3B2 cell line. To further examine the impact of genetic background after a mutation in a CDG, comparisons between multiple cell lines is necessary. While only one cell line was used in this experiment, we did create other cell lines that had the same deletion. Further comparisons between all of the created cell lines can examine how a genetic background can alter itself to enhance cancer survival.

Understanding how cancer evolves over time and its ability to obtain gain of function mutations is still being researched. Past studies have shown that cancer arises through mutations in CDGs and the impact of genetic background (Bailey et al., 2018). p53, a common CDG, is seen to be heavily mutated in most cancers (Hsu, 1991). Despite being widely studied, most studies in p53 have been done in a heterogeneous background. These results while valuable, ignore the effect that genetic background has on oncogenesis. A recent study demonstrated that functionally significant mutations in genetic background that occur after major mutations in CDGs can impact how cancer develops (Gerstung et al., 2020). The created mutant cell lines from this study sets up an ideal experimental setting to test how genetic background can influence cancer progression and evolution. The next steps are to allow for the cell lines to continue growing for over a year, then examine protein and RNA levels as well as growth rates and apoptotic function to determine how genetic background impacted the cells. The hope is that the genetic background will mutate to give cancer gain of function abilities. Better understanding of cancer evolution may help how cancer is treated in the future.

CHAPTER 4. CONCLUSIONS

Our experiment using CRISPR-Cas9 created a LOF deletion mutation in exon 4 of p53. Lower protein and RNA expression along with higher growth and lower apoptotic function was seen in the mutant cell line. Our results indicate LOF mutations mapping to CDGs such as p53 are of primary functional significance to cancer onset and progression. In addition, all the results of our experiment were completed in a genetically identical background, ensuring that changes are solely because of the created mutation.

However, recent genomic studies indicate that functionally significant changes in genetic backgrounds may arise subsequently to mutations in CDGs that further enhance cancer development. The recent paper by Gerstung et al. suggests that genetic background can undergo mutations that will lead to overall increased genomic stability in cells (2020). We believe that we have created an ideal experimental system for future studies on the evolution of secondary mutations (genetic background) occurring subsequent to an initiating mutation in a major cancer driver gene. By monitoring subsequent changes in genetic background in this strain over time, we hope to better understand how changes in genetic background of cancer cells can lead to cancer progression.

REFERENCES

- Antoun, S., Atallah, D., Tahtouh, R., Alaaeddine, N., Moubarak, M., Khaddage, A., Ayoub, E. N., Chahine, G., and Hilal, G. (2018). Different TP53 mutants in p53 overexpressed epithelial ovarian carcinoma can be associated both with altered and unaltered glycolytic and apoptotic profiles. *Cancer Cell International* 18, 14.
- Artimo P, J. M., Arnold K, Baratin D, Csardi G, de Castro E, Duvaud S, Flegel V, Fortier A, Gasteiger E, Grosdidier A, Hernandez C, Ioannidis V, Kuznetsov D, Liechti R, Moretti S, Mostaguir K, Redaschi N, Rossier G, Xenarios I, and Stockinger H. (2012). ExPASy: SIB bioinformatics resource portal. *Nucleic Acids Res.*
- Bailey, M. H., Tokheim, C., Porta-Pardo, E., Sengupta, S., Bertrand, D., Weerasinghe, A., Colaprico, A., Wendl, M. C., Kim, J., Reardon, B., Ng, P. K., Jeong, K. J., Cao, S., Wang, Z., Gao, J., Gao, Q., Wang, F., Liu, E. M., Mularoni, L., Rubio-Perez, C., ... Ding, L. (2018). Comprehensive Characterization of Cancer Driver Genes and Mutations. *Cell*, 173(2), 371–385.e18. <https://doi.org/10.1016/j.cell.2018.02.060>
- Balmain, A. (2002). Cancer as a Complex Genetic Trait: Tumor Susceptibility in Humans and Mouse Models. *Cell*, 198(2).
- Bossi, G., Lapi, E., Strano, S., Rinaldo, C., Blandino, G., & Sacchi, A. (2005, September 19). Mutant p53 gain of function: reduction of tumor malignancy of human cancer cell lines through abrogation of mutant p53 expression. Retrieved from <https://www.nature.com/articles/1209026>
- Brown, J. M., & Wouters, B. G. (1999, April). Apoptosis, p53, and Tumor Cell Sensitivity to Anticancer Agents. Retrieved from <https://pdfs.semanticscholar.org/b3da/c7e1e4b5aaa45529db5d5d97dfebb9a04deb.pdf>

- Das, P., Kotilingam D., Fau-Korchin, B., Korchin, B., Fau-Liu, J., Liu J., Fau-Yu, D., Yu D., Fau-Lazar, A. J., Lazar, Aj., Fau-Pollock, R.E., Pollock Re Fau - Lev, D., and Lev, D. High prevalence of p53 exon 4 mutations in soft tissue sarcoma.
- Dasari, S., & Tchounwou, P. B. (2014). Cisplatin in cancer therapy: molecular mechanisms of action. *European journal of pharmacology*, 740, 364–378.
<https://doi.org/10.1016/j.ejphar.2014.07.025>
- Donehower, L. A., Harvey, M. J., Vogel, H. A., McArthur, M. J., Montgomery, C., Thompson, T., and Bradley, A. (2006, July 20). Effects of genetic background on tumorigenesis in p53-deficient mice. Retrieved from
<https://onlinelibrary.wiley.com/doi/abs/10.1002/mc.2940140105?sid=nlm:pubmed>
- Florijan, M. K., Ozretić, P., Bujak, M., Pezzè, L., Ciribilli, Y., Kaštelan, Ž., Hudolin, T. (2019, April 2). The role of p53 isoforms' expression and p53 mutation status in renal cell cancer prognosis. Retrieved from
<https://www.sciencedirect.com/science/article/pii/S1078143919301000?via=ihub>
- Garcia-Martin, J. A., & Clote, P. (2015). RNA Thermodynamic Structural Entropy. *PloS one*, 10(11), e0137859. <https://doi.org/10.1371/journal.pone.0137859>
- Gerstung, M., Jolly, C., Leshchiner, I., D'Antonio, S. C., Gonzalez, S., Rosebrock, D., et al., (2020, February 6). The evolutionary history of 2,658 cancers. Retrieved from
<https://www.nature.com/articles/s41586-019-1907-7#citeas>
- Hanahan, D., and Weinberg, Robert A. (2011). Hallmarks of Cancer: The Next Generation. *Cell* 144, 646-674.
- Harris, S. L., & Levine, A. J. (2005). The p53 pathway: positive and negative feedback loops. *Oncogene*, 24(17), 2899–2908. doi: 10.1038/sj.onc.1208615

- Hsu, I. C., Metcalf, R. A., Sun, T., Welsh, J. A., Wang, N. J., & Harris, C. C. (1991). Mutational hot spot in the p53 gene in human hepatocellular carcinomas. *Nature*, 350(6317), 427–428. doi: 10.1038/350427a0
- Institute for Theoretical Chemistry at University of Vienna. (2019, August 13). RNAfold. Retrieved from <http://rna.tbi.univie.ac.at/cgi-bin/RNAWebSuite/RNAfold.cgi>
- Levine, A. J. (1997). p53, the Cellular Gatekeeper for Growth and Division. *Cell*, 88(3).
- Mittal, V. K., & McDonald, J. F. (2015). Integrated sequence and expression analysis of ovarian cancer structural variants underscores the importance of gene fusion regulation. *BMC medical genomics*, 8, 40. doi:10.1186/s12920-015-0118-9
- Muller, P. A. J., and Vousden, K. H. (2013). p53 mutations in cancer. *Nature Cell Biology* 15, 2.
- National Cancer Institute. (2015, February 9). What Is Cancer? Retrieved from <https://www.cancer.gov/about-cancer/understanding/what-is-cancer>
- O'Brien J et al. (2003). Investigation of the Alamar Blue (resazurin) fluorescent dye for the assessment of mammalian cell cytotoxicity. *The FEBS Journal*, 267, 5421-5426
- Olivier, M., Hollstein, M., & Hainaut, P. (2010). TP53 mutations in human cancers: origins, consequences, and clinical use. *Cold Spring Harbor perspectives in biology*, 2(1), a001008. doi:10.1101/cshperspect.a001008
- Pecorino, L. (2016). *Molecular Biology of Cancer: Mechanisms, Targets and Therapeutics* (4th ed.): Oxford University Press.
- Pellicciotta, I., Yang, C.-P. H., Venditti, C. A., Goldberg, G. L., & Shahabi, S. (2013). Response to microtubule-interacting agents in primary epithelial ovarian cancer cells. *Cancer Cell International*, 13(1), 33. doi:10.1186/1475-2867-13-33

- Radhakrishnan, S. K., & Gartel, A. L. (2006, March). CDK9 phosphorylates p53 on serine residues 33, 315 and 392. Retrieved from <https://www.ncbi.nlm.nih.gov/pubmed/16552184>
- Ratan, Z. A., Son, Y. J., Haidere, M. F., Uddin, B., Yusuf, M. A., Zaman, S. B., Kim, J. H., Banu, L. A., & Cho, J. Y. (2018). CRISPR-Cas9: a promising genetic engineering approach in cancer research. *Therapeutic advances in medical oncology*, 10, 1758834018755089. <https://doi.org/10.1177/1758834018755089>
- Rivlin, N., Brosh, R., Oren, M., and Rotter, V. (2011). Mutations in the p53 Tumor Suppressor Gene: Important Milestones at the Various Steps of Tumorigenesis. *Genes Cancer* 2, 466-474.
- Sanchez-Prieto, R., Rojas, J. M., Taya, Y., & Gutkind, J. S. (2000, May 1). A role for the p38 mitogen-activated protein kinase pathway in the transcriptional activation of p53 on genotoxic stress by chemotherapeutic agents. Retrieved from <https://www.ncbi.nlm.nih.gov/pubmed/10811125>
- Satpathy, M., Mezencev, R., Wang, L., and McDonald, J. F. (2016). Targeted in vivo delivery of EGFR siRNA inhibits ovarian cancer growth and enhances drug sensitivity. *Scientific Reports* 6, 36518.
- Sievers, F., Wilm, A., Dineen, D., Gibson, T. J., Karplus, K., Li, W., Higgins, D. G. (2011). Fast, scalable generation of high-quality protein multiple sequence alignments using Clustal Omega. *Molecular Systems Biology*, 7(1), 539. doi: 10.1038/msb.2011.75
- Shepherd, T., Tolbert, D., Benedetti, J., Macdonald, J., Stemmermann, G., Wiest, J., Fenoglio-Preiser, C. et al., (2005, October 27). Alterations in exon 4 of the p53 gene in gastric carcinoma. Retrieved from <https://www.ncbi.nlm.nih.gov/pubmed/10833478>

- Synthego. (2019). Full Stack Genome Engineering. Retrieved from <https://www.synthego.com/products/crispr-kits/gene-knockout-kit>
- Takara. (2020). How to design sgRNA sequences. Retrieved from <https://www.takarabio.com/learning-centers/gene-function/gene-editing/gene-editing-tools-and-information/how-to-design-sgrna-sequences>
- Ventura, A., Kirsch, D. G., McLaughlin, M. E., Tuveson, D. A., Grimm, J., Lintault, L., Jacks, T., et. al., (2007). Restoration of p53 function leads to tumour regression in vivo. *Nature Letters*.
- Vugt, M. A. V., Bràs, A., & Medema, R. H. (2005). Restarting the Cell Cycle When the Checkpoint Comes to a Halt. *Cancer Research*, 65(16), 7037–7040. doi: 10.1158/0008-5472.can-05-1054
- World Health Organization. (2020). Cancer. Retrieved from https://www.who.int/health-topics/cancer#tab=tab_1
- Yogosawa, S., & Yoshida, K. (2018). Tumor suppressive role for kinases phosphorylating p53 in DNA damage-induced apoptosis. *Cancer science*, 109(11), 3376–3382. <https://doi.org/10.1111/cas.13792>
- Yue, X., Zhao, Y., Xu, Y., Zheng, M., Feng, Z., & Hu, W. (2017, April 6). Mutant p53 in Cancer: Accumulation, Gain-of-Function, and Therapy. Retrieved from <https://www.sciencedirect.com/science/article/pii/S0022283617301638>
- Zhu, J., Zhou, W., Jiang, J., & Chen, X. (1998). Identification of a Novel p53 Functional Domain That Is Necessary for Mediating Apoptosis. *Journal of Biological Chemistry*, 273(21), 13030–13036. doi: 10.1074/jbc.273.21.13030

Zilfou, J. T., and Lowe, S. W. (2009). Tumor suppressive functions of p53. Cold Spring Harb Perspect Biol 1, a001883-a001883.

Zuker, M., & Stiegler, P. (1981). Optimal computer folding of large RNA sequences using thermodynamics and auxiliary information. *Nucleic acids research*, 9(1), 133–148.
<https://doi.org/10.1093/nar/9.1.133>